







Feedback cooling a levitated nanoparticle's libration to below 100 phonons

Jialiang Gao ^{1,2,*}, Fons van der Laan ^{1,2,3,*}, Joanna A. Zielińska ^{1,2}, Andrei Militaru ^{1,2},
Lukas Novotny ^{1,2} and Martin Frimmer ^{1,2}

¹Photonics Laboratory, *ETH Zürich*, 8093 Zürich, Switzerland

²Quantum Center, *ETH Zürich*, 8093 Zürich, Switzerland

³Center for Nanophotonics, *AMOLF*, 1098 XG Amsterdam, The Netherlands



(Received 29 February 2024; accepted 7 June 2024; published 1 July 2024)

Macroscopic rotors are interesting model systems to test quantum theory and for quantum sensing. A promising approach for bringing these systems to the quantum regime is to combine sensitive detection with feedback cooling to reduce the thermal occupation of the mechanics. Here, we implement a backward-scattering scheme to efficiently detect all three libration modes of an optically levitated nanoparticle. We demonstrate parametric feedback cooling of all three libration degrees of freedom to below 16 mK, with one of the modes reaching the temperature of 1.3 mK, corresponding to a mean phonon number of 84. Finally, we characterize the backward-scattering scheme by determining its measurement efficiency to be 0.5%.

DOI: [10.1103/PhysRevResearch.6.033009](https://doi.org/10.1103/PhysRevResearch.6.033009)

I. INTRODUCTION

Levitodynamics is the field of controlling levitated macroscopic objects. In the absence of a mechanical clamping mechanism, their motion can be highly isolated from the environment. Consequently, this platform is a prime candidate for studying macroscopic quantum dynamics as well as for sensing small forces and torques [1]. A milestone towards demonstrating quantum phenomena in levitation was reached by cooling the center-of-mass (c.m.) motion of an optically trapped particle to its ground state, both via coherent scattering into an optical cavity [2–4] and via measurement-based feedback [5–7].

Besides studying translational motion, levitated anisotropic particles are especially suited for exploring the control of rotational degrees of freedom. Rotational motion is particularly enticing in the quantum regime since it is intrinsically nonlinear and allows for unique quantum interference effects such as orientational quantum revivals [8]. Remarkable experimental progress has been made in rotational levitodynamics. On the one hand, levitated nanoparticles have been driven into rotation at gigahertz frequencies [9–12], and fluctuations of rotation rate have been controlled [13–15]. On the other hand, a restoring torque on the orientation creates libration modes, which behave like harmonic oscillators for small angular displacements. Cooling several libration modes simultaneously has been successfully demonstrated using a cavity [16] as well as measurement-based feedback [17,18]. Furthermore,

measurement backaction has been observed on optically levitated rotors [19]. However, a detection scheme with a sufficiently high efficiency for quantum control is still to be demonstrated [20].

While the first wave of experiments in rotational levitodynamics used cylindrically symmetric rotors (termed nanodumbbells), it became clear that they suffer from degenerate libration modes and their uncontrolled coupling by thermally driven spinning [17,19,21,22]. As a result, the attention of the community has recently shifted towards controlling all six degrees of freedom of fully anisotropic particles with three distinct moments of inertia [16,18]. These rotors exhibit nondegenerate libration modes, making each mode individually addressable in the frequency domain. A particularly tantalizing example of a rotational quantum effect (without counterpart in translational motion) requiring such an anisotropic rotor is quantum tennis-racket flips [23]. One requirement for their observation is sufficient cooling of the libration modes. Interestingly, recent experiments underline that control of librational motion is also key to sensitive experiments on the c.m. motion of levitated particles [7]. The further development of detection and cooling schemes for librational motion, especially of fully anisotropic levitated rotors, is thus of significant relevance to the entire levitodynamics community.

In this work, we use measurement-based parametric feedback cooling to control the orientation of a nanoparticle with three distinct moments of inertia. All three nondegenerate libration modes are cooled to below 16 mK, with the temperature of the coldest mode reaching 1.3 mK, corresponding to a mean phonon occupation of 84. Our approach relies on a back-scattering measurement scheme to enhance the detection efficiency by 3 orders of magnitude compared to its forward-scattering counterpart. Additionally, we experimentally determine the measurement efficiency $\eta = 0.5\%$ for the coldest libration mode in our system.

*These authors contributed equally to this paper.

Published by the American Physical Society under the terms of the [Creative Commons Attribution 4.0 International](https://creativecommons.org/licenses/by/4.0/) license. Further distribution of this work must maintain attribution to the author(s) and the published article's title, journal citation, and DOI.

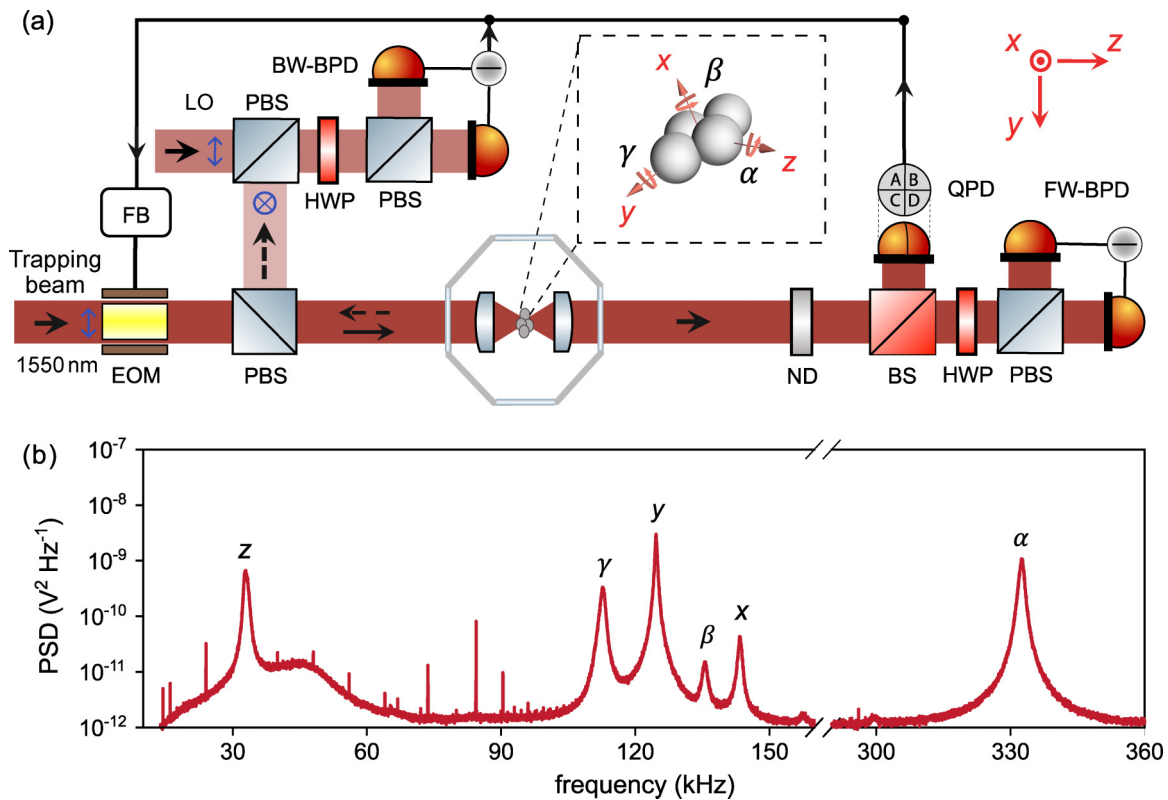


FIG. 1. (a) Schematic of the experimental setup. Inside a vacuum chamber, we generate an optical trap by strongly focusing a laser beam (propagating along z and linearly polarized along y). In the forward (FW) direction, we detect the particle’s c.m. motion on a quadrant photodetector (QPD) and libration motion on a balanced photodetector (FW-BPD). In the backward (BW) direction, the scattered light from the particle is overlapped with a local oscillator (LO) on another balanced photodetector (BW-BPD) for efficient detection of the libration modes. We use the signals from the QPD and the BW-BPD to modulate the power of the laser with an electro-optic modulator (EOM) for feedback cooling c.m. motion and librational motion, respectively. Inset: Illustration of a possible realization of an anisotropic particle with three distinct moments of inertia. The orientation of the particle is confined with its long axis along the polarization (y) axis and its mid-axis along the laser propagation (z) axis. Three libration modes, α , β , and γ , rotate the particle around the z , x , and y axes, respectively. (b) Power spectral density (PSD) of the signal measured by the FW-BPD at 0.8 mbar. The six labeled peaks correspond to the particle’s c.m. (x , y , z) and libration (α , β , γ) modes, respectively. The additional spikes are electronic noise from our detectors and the data acquisition card.

II. EXPERIMENTAL SETUP

We show our experimental setup in Fig. 1(a). The trapping beam [wavelength 1550 nm, optical power 900(50) mW], propagates along the z axis and is linearly polarized along the y axis. Inside a vacuum chamber, we form an optical trap by strongly focusing the beam with an aspheric lens ($NA = 0.69$). We trap a particle in the focus and collect its scattered light in the backward (BW) and forward (FW) direction using the trapping lens and a second, identical lens, respectively. We will return to details about the trapped particle and the trapping procedure shortly. In the forward direction, the scattered light, together with the trapping beam, is recollimated and half of the light is sent to a quadrant photodetector (QPD) for c.m. motion detection. For libration detection, the other half is distributed on a balanced photodetector (FW-BPD) using a half-wave plate (HWP) and polarizing beam splitter (PBS). In this forward detection scheme, the trapping beam is automatically overlapped with the scattered light and acts as a local oscillator. This makes the detection scheme robust against drift and straightforward to implement. However, we have to attenuate the light (and therefore also the signal) on

the detectors with a neutral density filter (ND, transmission 0.2%) to avoid damage to the detectors from the high power of the trapping beam. A spectrum recorded by the FW-BPD at 0.8 mbar is shown in Fig. 1(b). The spectrum shows three c.m. modes (x , y , z) and three libration modes (α , β , γ), indicating a trapped particle with three distinct moments of inertia. To increase the detection efficiency of the libration mode in the polarization plane of the optical trap (characterized by the angle α), we implement an additional back-scattering detection scheme as proposed in Ref. [24]. To understand the principle of the libration detection mechanism, consider a particle with its long axis aligned with the polarization axis of the light field (y axis). Due to the particle’s anisotropic polarizability, any deviation from this alignment by an angle α in the focal plane induces an x -polarized dipole in the particle. This dipole’s amplitude, and therefore also its radiated field, scales linearly with α (for $\alpha \ll 1$). To detect this field in the backward direction, we select the x -polarized scattered light using a PBS and overlap the light with a local oscillator (LO, optical power ~ 5 mW) in a heterodyne measurement using another HWP, a PBS, and a balanced photodetector (BW-BPD). The LO is produced as a small portion split from the main trapping beam,

and its frequency is shifted by 9 Hz from that of the trapping beam. Since this frequency difference is much smaller than the linewidths of the motional peaks, the motional sidebands are effectively overlapped in a single-sided power spectral density without significant additional broadening. With this method, we circumvent having to phase lock the LO at the cost of halving the signal strength. The back-scattering scheme requires no light attenuation, since we independently control the power of the LO.

To stabilize the particle inside the trap, we perform parametric feedback cooling on all translational and librational degrees of freedom using the signals from the QPD (for c.m. motion) and the BW-BPD (for libration) [21,25]. Parametric feedback cooling of a harmonic oscillator relies on modulating its resonance frequency at twice the eigenfrequency with a phase suitably locked to the oscillator's motion [25]. In our experiment, for each degree of freedom (c.m. and libration), a phase-locked loop (PLL) tracks frequency and phase of the measured signal. The feedback signal is the frequency-doubled output of the PLL with appropriately adjusted phase [26]. The sum of all feedback signals is applied to an electro-optic modulator (EOM), modulating the trapping beam power which in turn leads to a modulation of the eigenfrequencies of the modes. Given that all oscillation modes of the particle are nondegenerate, with the frequency differences largely exceeding the linewidths, this method can effectively address all modes individually in frequency space and therefore cool them all simultaneously [19,26,27].

We load silica spheres (nominal diameter of 156 nm, dispersed in isopropanol) into the trap using a nebulizer. By controlling the concentration of silica spheres in the initial solution, some spheres aggregate to form nanoclusters. The solution therefore contains single spheres, nanodumbbells, and other nanoclusters with complex shapes, such as anisotropic particles with three different moments of inertia. Indeed, we also trap particles in the shape of individual spheres and dumbbells in our experiments. However, based on the number of librational motion peaks in the PSD, we exclude single spheres (no librational motion peak) and dumbbells (two librational motion peaks) and select only the particles having three distinct librational motion peaks. Although we cannot control the exact shape of each trapped particle, we are able to repeatably trap particles with three librational motion peaks. The exact motional frequencies slightly differ from particle to particle by a few tens of kilohertz. All experiments in this work are performed with the same particle. A possible example of an anisotropic particle with three different moments of inertia is illustrated in the inset of Fig. 1(a).

Let us turn our attention to the orientation of the particle in the trap. The observation of three libration modes in Fig. 1(b) indicates that the orientation is fully confined in three dimensions. Note that, when trapped in a purely linearly polarized light field, the orientation of an anisotropic point scatterer is expected to exhibit only two confined libration modes (along with one unconfined degree of freedom corresponding to free rotation around the long axis) [17,21,28,29]. We conjecture that the complete six-dimensional confinement observed in this work is a consequence of the additional orientation confinement mechanism due to the intensity gradient of the trap [18,30]. Following the arguments presented in Ref. [18], we

expect the combination of the trapping beam's polarization and intensity gradient to result in the longest axis of the particle aligning along the polarization (y) axis, and the mid-axis along the laser propagation (z) axis, as illustrated by the inset of Fig. 1(a). Another hint supporting our conjecture of the particle's orientation comes from the damping rates of the c.m. motion. The findings of Ref. [10] indicate that the larger the cross section of an irregularly shaped particle is when projected along a particular direction, the larger the damping rate is for linear motion along that direction. We therefore determine the damping rate for linear motion by fitting the c.m. motion peaks in the PSD [shown in Fig. 1(b)] with Lorentzian functions and extract their respective linewidths γ_x , γ_y , and γ_z . In our experiment, we find $(\gamma_x : \gamma_z : \gamma_y = 1.7 : 1.3 : 1)$. The order of the damping rates $\gamma_x > \gamma_z > \gamma_y$ supports the conjecture that the particle orientation is, indeed, as illustrated in the inset of Fig. 1(a).

III. LIBRATION DETECTION AND COOLING

Having identified the three libration modes, we turn our attention to comparing the forward and backward detection schemes. Since the optical powers on the FW-BPD and the BW-BPD are unequal and the detectors have different transimpedance gains, we normalize the obtained libration spectra to their respective noise floors. In Fig. 2(a), we show the power spectral densities of the α (light blue), β (red), and γ (dark blue) modes recorded on the BW-BPD at 0.8 mbar. As dashed lines, we show the corresponding modes simultaneously recorded on the FW-BPD. We observe that the signal-to-noise ratio of the BW-BPD exceeds that of the FW-BPD by approximately 3 orders of magnitude for all libration modes. We mainly attribute this increase in signal to the reduction of light attenuation in the backward direction in comparison to the forward direction, where the ND filter introduces a loss of signal of 3 orders of magnitude.

We continue by exploiting the signal detected by the BW-BPD to perform PLL feedback cooling on all three libration modes between 10^{-3} and 10^{-8} mbar. Figure 2(b) shows the power spectral densities for the α , β , and γ modes at 3×10^{-8} mbar. Again, the solid lines are recorded using the BW-BPD and the dashed lines are recorded using the FW-BPD. We fit the peak of each mode to a Lorentzian function. By integrating the area under the peak of each mode and subtracting the noise floor, we extract the effective temperature of each libration mode [31]. Figure 2(c) shows the measured temperature as a function of pressure of the three libration modes under feedback cooling. For pressures above 10^{-7} mbar, the temperatures of all three modes decrease linearly with pressure. However, between 10^{-8} and 10^{-7} mbar, the temperatures of the α and β modes level off, indicating that they are no longer limited by pressure [26]. Note that, at 3×10^{-8} mbar, the settings of the feedback for the α mode are optimized. We summarize the measured temperatures and mean phonon occupation numbers at the lowest pressure of 1.3×10^{-8} mbar in Table I. Our detection scheme is optimized for the α mode (libration in the focal plane of the optical trap) [24]. We indeed find the lowest phonon occupation of 84 for that mode. We stress that, under feedback cooling at low pressures, the libration peaks are not discernible above the noise floor on

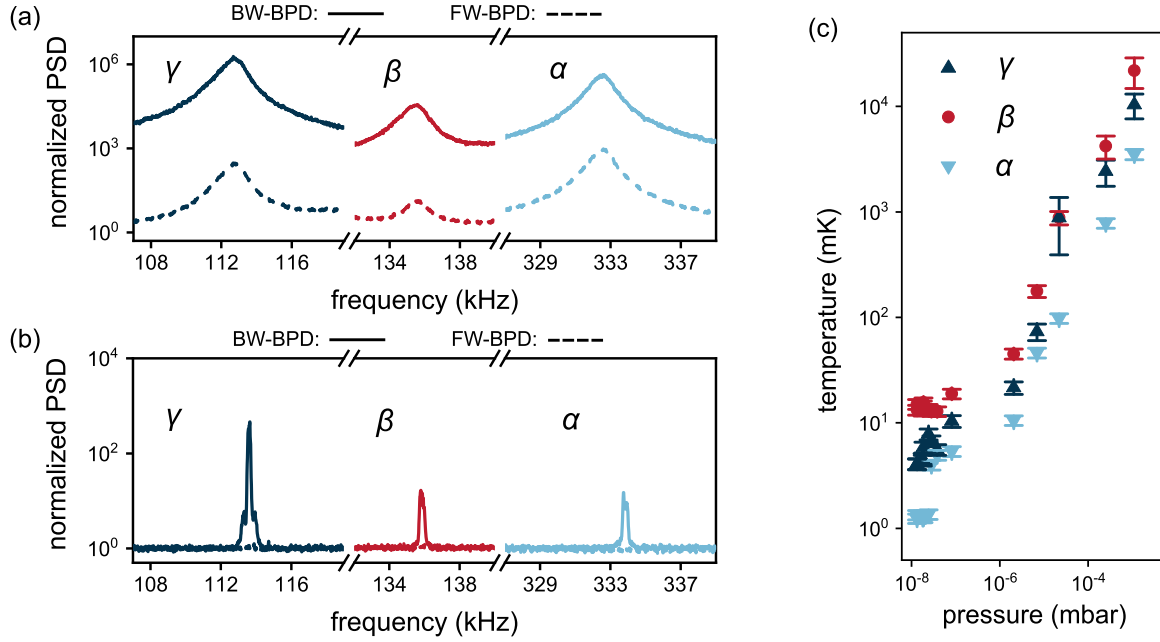


FIG. 2. (a) Comparison of forward and backward detection. Normalized power spectral densities (PSD) of the libration modes α (light blue), β (red), and γ (dark blue) at 0.8 mbar. The spectra recorded on the backward detector (BW-BPD, solid lines) and forward detector (FW-BPD, dashed lines) are normalized to their respective noise floor in order to compare their signal-to-noise ratios. (b) Normalized power spectral densities of the same libration modes as in panel (a) under feedback cooling at 3×10^{-8} mbar. (c) Temperature of the three libration modes as a function of pressure measured under parametric feedback cooling. At 3×10^{-8} mbar, the settings of the feedback for the α mode are optimized. The recorded data are based on the backward detection. Error bars represent the standard deviation of the fit.

the FW-BPD, as seen in Fig. 2(b). Thus, feedback cooling using the forward detection would not have been able to reach similar temperatures.

IV. MEASUREMENT EFFICIENCY

Having exploited the signal from our backward detection scheme for parametric feedback cooling, let us turn to characterizing our detection system in more depth. The figure of merit of paramount importance in the context of quantum measurements is the measurement efficiency η , which describes how far from optimal a measurement system is. Here, optimal means that the imprecision-backaction product is saturated at the limit set by the Heisenberg uncertainty relation. To be concrete, for a librator whose orientation is monitored, the imprecision-backaction product reads $\tilde{S}_{\tau\tau}\tilde{S}_{\text{imp}}\eta = \hbar^2$, with \hbar being the reduced Planck constant. Here, $\tilde{S}_{\tau\tau}$ is the single-sided power spectral density of the torque fluctuations driving the libration mode [32]. Furthermore, \tilde{S}_{imp} is the measurement imprecision of the orientation angle of the librator. In the

optimal case ($\eta = 1$), the torque fluctuations $\tilde{S}_{\tau\tau}$ arise purely from measurement backaction (i.e., radiation torque shot noise), while the measurement imprecision \tilde{S}_{imp} is minimized by optimally detecting all scattered light holding information about the librator's orientation. Both excess backaction (e.g., from collisions with gas molecules) and excess imprecision (e.g., from the finite quantum efficiency of the photodetector or from a finite collection efficiency of the optics) reduce the measurement efficiency to below unity ($\eta < 1$). In the following, we experimentally determine the measurement efficiency of our system.

To this end, we measure both the total backaction $\tilde{S}_{\tau\tau}$ and the total imprecision \tilde{S}_{imp} . The measurement imprecision is directly given by $\tilde{S}_{\text{imp}} = \tilde{S}_{\text{imp}}^{\text{exp}}/c^2$, where $\tilde{S}_{\text{imp}}^{\text{exp}}$ is the detector noise floor in V^2/Hz and c is the calibration factor in V/rad , which is determined from the equipartition theorem $c^2 = I\Omega_\alpha^2 \langle v_{\text{cal}}^2 \rangle / (k_B T_{\text{cal}})$, with k_B being the Boltzmann constant. Here, $\langle v_{\text{cal}}^2 \rangle$ is found during a calibration measurement at known temperature T_{cal} by integrating the measured power spectral density (in units of V^2/Hz) [31]. In order to determine $\tilde{S}_{\tau\tau}$, we perform reheating measurements of the libration mode α and extract the reheating rate at different pressures [19]. At the start of each iteration of the reheating protocol, feedback cooling of the mode α is turned off for 0.6 s, after which feedback cooling is turned on again. We demodulate the libration signal with a bandwidth of 4 kHz with a lock-in amplifier to continuously measure the energy of the libration mode (in units of V^2). Part of a typical timetrace of the libration energy is shown in Fig. 3(a). The protocol is repeated 50 times and the stochastic reheating trajectories are averaged, as shown

TABLE I. Measured temperatures and mean phonon occupations for each libration mode at 1.3×10^{-8} mbar. Errors are given as 1 standard deviation.

Mode	Temperature (mK)	Occupation
α	1.34 ± 0.14	84 ± 9
β	15 ± 2	2298 ± 248
γ	4.1 ± 0.5	742 ± 87

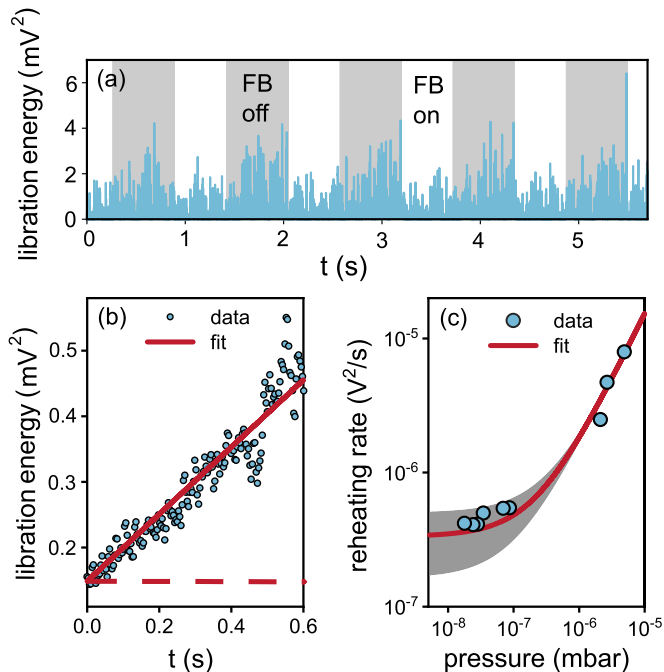


FIG. 3. (a) During the reheating protocol the feedback cooling is toggled on (white areas) and off (gray areas), while we measure the energy of the α mode in mV^2 . (b) Energy (in units of detector signal variance mV^2) as a function of time at 7×10^{-8} mbar after switching off the parametric feedback cooling. The data are averaged over all 50 cycles. A linear fit to the data is shown as the red solid line. The average energy under continuous feedback cooling is shown as the dashed line. (c) Heating rate (blue circles) as a function of pressure. A linear fit to the data is shown as the red solid line. The shaded area represents 1 standard deviation of the fit.

in Fig. 3(b). As expected, for timescales much shorter than the damping time, the energy increases linearly in time. We extract the heating rate Γ^{exp} (in units of V^2/s) as the slope from a linear fit shown as the solid line in Fig. 3(b). We constrain the fit at $t = 0$ to be equal to the average energy under continuous feedback cooling, indicated by the dashed line. In Fig. 3(c) we plot the heating rate measured at different pressures. As expected, the heating rate decreases linearly with pressure until it saturates at 10^{-8} mbar [19]. We fit $\Gamma^{\text{exp}} = a \times p_{\text{gas}} + \Gamma_{\text{res}}^{\text{exp}}$ to our data with the scaling a and the residual damping rate $\Gamma_{\text{res}}^{\text{exp}}$ as fit parameters. The fit and the corresponding uncertainty are depicted as a solid line and a shaded region, respectively. Using the fit, we determine the heating rate $\Gamma^{\text{exp}} = 3.5 \times 10^{-7} \text{V}^2/\text{s}$ at 1.3×10^{-8} mbar. As a last step, we apply the fluctuation-dissipation theorem to find $\tilde{S}_{\tau\tau} = 4I^2\Omega_\alpha^2\Gamma^{\text{exp}}/c^2$, where I is the moment of inertia corresponding to mode α , and Ω_α is its eigenfrequency. By rewriting the imprecision-backaction product, we find the measurement efficiency expressed in experimentally measurable quantities as

$$\eta = \left(\frac{\hbar}{2}\right)^2 \frac{\Omega_\alpha^2 \langle v_{\text{cal}}^2 \rangle^2}{(k_B T_{\text{cal}})^2} \frac{1}{\Gamma^{\text{exp}} \tilde{S}_{\text{imp}}^{\text{exp}}}. \quad (1)$$

Note that the moment of inertia does not appear in Eq. (1). Thus, we can determine the measurement efficiency without

the knowledge of the exact shape of the trapped particle. For our current setup, we extract the measurement efficiency for the α mode to be $\eta = 0.5\%$. The maximum achievable detection efficiency using a lens with $\text{NA} = 0.69$ is $\eta_{\text{det}} = 20\%$ [24]. At low pressures, we can assume that the dominant contribution to $\tilde{S}_{\tau\tau}$ is from quantum backaction (radiation torque shot noise) [19]. Accordingly, our measurement efficiency is currently limited by excess imprecision contributing to \tilde{S}_{imp} , which we attribute to the limited mode overlap with the Gaussian mode of the fiber-coupled detector, sweeping the phase of the LO instead of locking it, and contributions of electronic noise.

V. CONCLUSION

In conclusion, we have parametrically feedback cooled all three libration modes of an optically levitated anisotropic nanoparticle from room temperature to below 16 mK. In particular, we obtained a record-low phonon occupation of 84 phonons for the libration mode in the focal plane of the optical trap. In order to reach this cooling performance, we implemented a backward scattering detection scheme. Even though the scheme is optimized for detecting libration in the focal plane, the other two libration modes are also clearly visible. We have observed an increase in detection efficiency of approximately 3 orders of magnitude for all libration modes for the backward detection scheme, compared with the commonly used forward scattering scheme. The backward detection scheme implemented in this work, together with the anisotropic nature of the trapped nanoparticle, allowed for feedback cooling to a level that represents an important step towards rotational quantum experiments [33]. One requirement to observe quantum tennis-racket flips is to prepare the initial state of a nanoparticle according to the relation $\hbar\omega/k_B T \geq 0.1$, where ω is the angular velocity of rotation around the mid-axis of the nanoparticle, and T is the effective temperature of the libration motion along the mid-axis [23]. For the nanoparticle cooled as described in this study, achieving the required initialization involves a moderate mid-axis rotation rate in the megahertz range, which is within experimental reach [9,10].

For applications requiring even lower phonon occupations, we envision two strategies to improve cooling performance. The first strategy is to further optimize the measurement efficiency. To this end, it will be crucial to maximize the mode overlap of the backscattered light with the LO on the BW-BPD and to lock the phase of the LO for a true homodyne detection scheme. The second strategy to reach lower phonon occupations is to switch from parametric feedback cooling to linear feedback cooling (often termed ‘‘cold damping’’ [34]), which has been empirically found to outperform parametric cooling (at fixed measurement efficiency) [5,6]. In particular, for cold damping, the minimal phonon occupation achievable only depends on the measurement efficiency according to $\bar{n}_{\text{min}} = (1/\sqrt{\eta} - 1)/2$. Given the measurement efficiency $\eta = 0.5\%$ determined for our system in this work, we expect $\bar{n}_{\text{min}} = 6.4$. Accordingly, when equipped with linear feedback cooling, our system will be able to perform sideband thermometry of a libration mode [35–37]. The principle of linear feedback cooling of a libration mode has been

demonstrated by applying the feedback torque both optically [17] and electrically [14,18]. We note that the improved performance of linear feedback cooling over parametric feedback comes at the price of giving up the robustness and simplicity of parametric feedback. If the linear feedback is effected via an electric field, the particle needs to be charged, making it susceptible to stray fields. Effecting the linear feedback via optical torques requires additional optical complexity, such as additional laser beams. Therefore, it depends on the application which feedback method is most suitable. For applications requiring extremely low phonon numbers, by carefully

minimizing the optical losses, ground state cooling of the librational mode appears within reach.

ACKNOWLEDGMENTS

We acknowledge our colleagues at the Photonics Laboratory at ETH Zürich for useful discussions. This research was supported by an ETH Research Grant (Grant No. ETH-385 47 20-2), the Swiss National Science Foundation (Grant No. 200021_212599), and the Swiss State Secretariat for Education, Research and Innovation (Grant No. UeM019-2).

-
- [1] C. Gonzalez-Ballester, M. Aspelmeyer, L. Novotny, R. Quidant, and O. Romero-Isart, Levitodynamics: Levitation and control of microscopic objects in vacuum, *Science* **374**, eabg3027 (2021).
- [2] U. Delić, M. Reisenbauer, K. Dare, D. Grass, V. Vuletić, N. Kiesel, and M. Aspelmeyer, Cooling of a levitated nanoparticle to the motional quantum ground state, *Science* **367**, 892 (2020).
- [3] A. Ranfagni, K. Børkje, F. Marino, and F. Marin, Two-dimensional quantum motion of a levitated nanosphere, *Phys. Rev. Res.* **4**, 033051 (2022).
- [4] J. Piotrowski, D. Windey, J. Vijayan, C. Gonzalez-Ballester, A. de los Ríos Sommer, N. Meyer, R. Quidant, O. Romero-Isart, R. Reimann, and L. Novotny, Simultaneous ground-state cooling of two mechanical modes of a levitated nanoparticle, *Nat. Phys.* **19**, 1009 (2023).
- [5] F. Tebbenjohanns, M. L. Mattana, M. Rossi, M. Frimmer, and L. Novotny, Quantum control of a nanoparticle optically levitated in cryogenic free space, *Nature (London)* **595**, 378 (2021).
- [6] L. Magrini, P. Rosenzweig, C. Bach, A. Deutschmann-Olek, S. G. Hofer, S. Hong, N. Kiesel, A. Kugi, and M. Aspelmeyer, Real-time optimal quantum control of mechanical motion at room temperature, *Nature (London)* **595**, 373 (2021).
- [7] M. Kamba and K. Aikawa, Revealing the velocity uncertainties of a levitated particle in the quantum ground state, *Phys. Rev. Lett.* **131**, 183602 (2023).
- [8] B. A. Stickler, B. Papendell, S. Kuhn, B. Schrinke, J. Millen, M. Arndt, and K. Hornberger, Probing macroscopic quantum superpositions with nanorotors, *New J. Phys.* **20**, 122001 (2018).
- [9] R. Reimann, M. Doderer, E. Hebestreit, R. Diehl, M. Frimmer, D. Windey, F. Tebbenjohanns, and L. Novotny, GHz rotation of an optically trapped nanoparticle in vacuum, *Phys. Rev. Lett.* **121**, 033602 (2018).
- [10] J. Ahn, Z. Xu, J. Bang, Y.-H. Deng, T. M. Hoang, Q. Han, R.-M. Ma, and T. Li, Optically levitated nanodumbbell torsion balance and GHz nanomechanical rotor, *Phys. Rev. Lett.* **121**, 033603 (2018).
- [11] J. Ahn, Z. Xu, J. Bang, P. Ju, X. Gao, and T. Li, Ultrasensitive torque detection with an optically levitated nanorotor, *Nat. Nanotechnol.* **15**, 89 (2020).
- [12] P. Ju, Y. Jin, K. Shen, Y. Duan, Z. Xu, X. Gao, X. Ni, and T. Li, Near-field GHz rotation and sensing with an optically levitated nanodumbbell, *Nano Lett.* **22**, 10157 (2023).
- [13] F. van der Laan, R. Reimann, A. Militaru, F. Tebbenjohanns, D. Windey, M. Frimmer, and L. Novotny, Optically levitated rotor at its thermal limit of frequency stability, *Phys. Rev. A* **102**, 013505 (2020).
- [14] C. P. Blakemore, D. Martin, A. Fieguth, N. Priel, G. Venugopalan, A. Kawasaki, and G. Gratta, Librational feedback cooling, *Phys. Rev. A* **106**, 023503 (2022).
- [15] S. Kuhn, B. A. Stickler, A. Kosloff, F. Patolsky, K. Hornberger, M. Arndt, and J. Millen, Optically driven ultra-stable nanomechanical rotor, *Nat. Commun.* **8**, 1670 (2017).
- [16] A. Pontin, H. Fu, M. Toroš, T. S. Monteiro, and P. F. Barker, Simultaneous cavity cooling of all six degrees of freedom of a levitated nanoparticle, *Nat. Phys.* **19**, 1003 (2023).
- [17] J. Bang, T. Seberon, P. Ju, J. Ahn, Z. Xu, X. Gao, F. Robicheaux, and T. Li, Five-dimensional cooling and nonlinear dynamics of an optically levitated nanodumbbell, *Phys. Rev. Res.* **2**, 043054 (2020).
- [18] M. Kamba, R. Shimizu, and K. Aikawa, Nanoscale feedback control of six degrees of freedom of a near-sphere, *Nat. Commun.* **14**, 7943 (2023).
- [19] F. van der Laan, F. Tebbenjohanns, R. Reimann, J. Vijayan, L. Novotny, and M. Frimmer, Sub-kelvin feedback cooling and heating dynamics of an optically levitated librator, *Phys. Rev. Lett.* **127**, 123605 (2021).
- [20] F. Tebbenjohanns, M. Frimmer, and L. Novotny, Optimal position detection of a dipolar scatterer in a focused field, *Phys. Rev. A* **100**, 043821 (2019).
- [21] T. Seberon and F. Robicheaux, Parametric feedback cooling of rigid body nanodumbbells in levitated optomechanics, *Phys. Rev. A* **99**, 013821 (2019).
- [22] J. A. Zielińska, F. van der Laan, A. Norrman, R. Reimann, M. Frimmer, and L. Novotny, Long-axis spinning of an optically levitated particle: A levitated spinning top, *Phys. Rev. Lett.* **132**, 253601 (2024).
- [23] Y. Ma, K. E. Khosla, B. A. Stickler, and M. S. Kim, Quantum persistent tennis racket dynamics of nanorotors, *Phys. Rev. Lett.* **125**, 053604 (2020).
- [24] F. Tebbenjohanns, A. Militaru, A. Norrman, F. van der Laan, L. Novotny, and M. Frimmer, Optimal orientation detection of an anisotropic dipolar scatterer, *Phys. Rev. A* **105**, 053504 (2022).
- [25] J. Gieseler, B. Deutsch, R. Quidant, and L. Novotny, Subkelvin parametric feedback cooling of a laser-trapped nanoparticle, *Phys. Rev. Lett.* **109**, 103603 (2012).
- [26] V. Jain, J. Gieseler, C. Moritz, C. Dellago, R. Quidant, and L. Novotny, Direct measurement of photon recoil from a levitated nanoparticle, *Phys. Rev. Lett.* **116**, 243601 (2016).

- [27] J. Vovrosh, M. Rashid, D. Hempston, J. Bateman, M. Paternostro, and H. Ulbricht, Parametric feedback cooling of levitated optomechanics in a parabolic mirror trap, *J. Opt. Soc. Am. B* **34**, 1421 (2017).
- [28] F. van der Laan, Rotational levitodynamics, Ph.D. thesis, ETH Zurich, 2022.
- [29] J. A. Zielińska, F. van der Laan, A. Norrman, M. Rimlinger, R. Reimann, L. Novotny, and M. Frimmer, Controlling optomechanical libration with the degree of polarization, *Phys. Rev. Lett.* **130**, 203603 (2023).
- [30] K. Zeng, J. Pu, X. Xu, Y. Wu, D. Xiao, and X. Wu, Gradient torque and its effect on rotational dynamics of optically trapped non-spherical particles in the elliptic Gaussian beam, *Opt. Express* **31**, 16582 (2023).
- [31] E. Hebestreit, M. Frimmer, R. Reimann, C. Dellago, F. Ricci, and L. Novotny, Calibration and energy measurement of optically levitated nanoparticle sensors, *Rev. Sci. Instrum.* **89**, 033111 (2018).
- [32] We define our power spectral densities according to $\langle \alpha^2 \rangle = \int_0^\infty \tilde{S}_{\alpha\alpha}(f) df$.
- [33] B. A. Stickler, K. Hornberger, and M. Kim, Quantum rotations of nanoparticles, *Nat. Rev. Phys.* **3**, 589 (2021).
- [34] F. Tebbenjohanns, M. Frimmer, A. Militaru, V. Jain, and L. Novotny, Cold damping of an optically levitated nanoparticle to microkelvin temperatures, *Phys. Rev. Lett.* **122**, 223601 (2019).
- [35] T. P. Purdy, P.-L. Yu, N. S. Kampel, R. W. Peterson, K. Cicak, R. W. Simmonds, and C. A. Regal, Optomechanical Raman-ratio thermometry, *Phys. Rev. A* **92**, 031802(R) (2015).
- [36] U. Delić, M. Reisenbauer, D. Grass, N. Kiesel, V. Vuletić, and M. Aspelmeyer, Cavity cooling of a levitated nanosphere by coherent scattering, *Phys. Rev. Lett.* **122**, 123602 (2019).
- [37] F. Tebbenjohanns, M. Frimmer, V. Jain, D. Windey, and L. Novotny, Motional sideband asymmetry of a nanoparticle optically levitated in free space, *Phys. Rev. Lett.* **124**, 013603 (2020).